Cleavage and Recovery of Molecular Water in Silica

Renée M. Van Ginhoven,[†,§,#] Hannes Jónsson,[‡,§,||] Byeongwon Park,[⊥,#] and L. René Corrales*[,#]

Department of Chemistry, University of Washington, Seattle, Washington 98195, Faculty of Science VR-II, University of Iceland, 107 Reykjavik, Iceland, Korean Institute of S&T Evaluation and Planning, Seoul, 137-130 Korea, and Pacific Northwest National Laboratory, PO Box 999, Richland, Washington 99352

Received: November 3, 2004; In Final Form: April 5, 2005

The network response associated with the incorporation and reactivity of water molecules in bulk phases of amorphous and crystalline silica are investigated using density functional theory. The extent of network relaxation is found to change the relative stabilities of the reactant and product states. A highly reactive site, with a low activation barrier, is associated with a highly strained site in which network relaxation significantly stabilizes the silanol state by effectively annealing the local structure. Diffusion and exchange reaction paths are found to likely be associated with minimum energy paths in which the stability of the product and reactant states are equal. These latter paths are associated with minimal network response, although the ability of the silanol groups to take on several conformations has an overall effect of changing the stability along a given reaction path.

1. Introduction

The reaction of molecular water with silica and its reverse reaction

$$\mathrm{SiOSi} + \mathrm{H_2O} \leftrightarrow 2\mathrm{SiOH} \qquad (1)$$

play key roles in the diffusion of water in silica,[2] in the processes that lead to dissolution or corrosion,[3] in the exchange of oxygen atoms with the network backbone,[4,5] in sol−gel processing,[6] and in controlling the phase stability of surfactant/silica composites.[7] The presence of water, either in the reacted form as silanol groups (Si−OH) or in its molecular form, has strong effects on the physical properties of silica. At elevated temperatures, the presence of water reduces the viscosity.[2] At lower temperatures, the presence of water can affect properties such as the optical absorption.[2] Experiments have characterized water reaction and diffusion into silica glass by determining the buildup of silanol groups and the extent of penetration,[1] the exchange of oxygen isotopes between labeled water and the silica network,[8,9] the solubility of water in silica and its dependence on vapor pressure and temperature of the system,[10] and by glass dissolution methods.[2] Other recent experiments include studies in which significant network relaxation or modification ensue from the reaction of water with silica at the surface as well as in the bulk[11,12] and when molecular water is solvated in silica.[13]

Silica glass is known to contain different concentrations of water in the form of silanol groups or whole molecular water. The concentration and distribution of water or silanol groups in a particular glass depends on the sample history. In fact, it is very difficult to make a dry glass without the use of additives such as fluorine. The mechanism for trapping reacted water in silica is difficult to determine experimentally because the reactions generally occur during processing and the water cannot be subsequently removed. In contrast, water can diffuse from the surface of a glass into its interior, and vice versa, and continue diffusing if it does not trap. The mechanism for diffusion consists of a mix of the water−silica reaction and its reverse and whole molecular water molecules diffusing through the open network structure without reactions. Experiments based on diffusion studies predict average reaction activation barriers of around 18 kcal/mol (0.78 eV).[1] The relationship between "trapped" water and diffusive water is not well known, and it is difficult to determine the mechanism of trapping experimentally. In this work, density functional theory (DFT) calculations are used to show that nondiffusive silanol groups are a result of an irreversible reaction that anneals the glass network to a significantly lower energy configuration. A comparison is made with a glass system in which diffusive behavior by a reaction mechanism is observed. Network relaxation is found to play a key role in controlling the height of the activation barriers by varying the degree of stability between the reactant and product states. Additionally, the possibility that the silanol state has multiple configurations caused by network response can lead to stabilizing that state, an effect not seen in pristine crystals.

The characterization of the reactivity of water with silica has received considerable theoretical attention. Previous theoretical studies of water interacting with silica focused on gas-phase cluster calculations that are unable to capture the effects of network response.[14−16] Earlier bulk-like calculations focused on the diffusion of water in large quartz-like clusters that allowed only the relaxation of the water molecules.[17] Additional studies of water binding in quartz have considered the importance of network response,[18] albeit still in large quartz-like clusters. Recent work has addressed key issues in diffusion and reactions of water with respect to different ring sizes and defects in silica.[19,20] That work mentioned the existence of a range of activation barriers and a range of relative stability between the molecular water and silanol states. The intent of this study is

* Corresponding author. E-mail: rene.corrales@pnl.gov.
† E-mail: rmvangi@sandia.gov.
‡ E-mail: hannes@u.washington.edu.
§ University of Washington.
|| University of Iceland.
⊥ Korean Institute of S&T Evaluation and Planning; e-mail: bpark@kistep.re.kr.
Pacific Northwest National Laboratory.

10.1021/jp044973n CCC: $30.25
Published on Web 05/06/2005

to uncover the source of the ranges of the activation barrier and relative stability as well as to reveal the role of network relaxation in the reaction pathways.

In contrast to the perfect crystalline states, amorphous silica has a medium-range structure with a wide range and distribution of ring sizes. The local molecular structure in terms of the Si−O bond lengths and O−Si−O bond angle of the fundamental SiO_4 tetrahedron are very similar for crystal and amorphous states, but distortions of the local structure can play an important role in reactivity. In amorphous systems, the Si−O−Si bond angle and the dihedral angle distributions are associated with different ring sizes and their conformations. A range of reaction barriers may, at least in part, correspond to different degrees of strain due to different ring sizes,[19,21−23] where the smaller rings are associated with greater local strain. In glass, strained sites can also manifest from contortions of larger rings. The quality of the glass structure plays a key role in its reactivity, and the reactivity of the nearby network can change after a reaction takes place.

The evidence of increased reactivity of small rings (containing three or four Si atoms) relative to larger rings is derived predominantly from studies of isolated rings in equilibrium conformations. The difference in strain due to ring size, however, does not explain the occurrence of extended network relaxation. The correlation of chemical reactivity with network relaxation requires an understanding of network connectivity and strain distribution. The relationship between the release (or increase) of strain upon reaction and its role in the relative stability between the reactants and products is unknown. Changes in the relative stability of reactants and products should be correlated with changes in the height of the reaction barrier.[24]

At dry silica surfaces, there can be surface reconstruction to form two-membered rings that quickly react with water. Two-membered rings are not likely to occur in the bulk at significant or measurable concentrations. The case of these very small rings is not discussed in this work. Reactions of water with two-membered rings and other strained configurations at surfaces of silica have been addressed by others.[23,25]

A full study would require that the reaction pathways be investigated for every site, but such a course is prohibitively computationally expensive. One simple solution is to add water across all of the SiO bonds, one at a time, to determine the relative stability. However, what is needed first is insight about the correlation between the reactant and product states and the local structure and response of the network. In glasses, the short-range structure may look similar at different points, but the associated intermediate-range structure may differ significantly. The latter difference will lead to a different response of the local network. Therefore, detailed reaction pathways are studied for a single site in each of two distinct glass samples that differ in their fundamental intermediate-range structure. The glass samples used here are prepared in an identical manner, but have very different structure features and differ in density. They are intended to be models of real glassy silica, but there are differences in simulated glasses and real glasses that are discussed elsewhere.[26] The key point here is that the two glass samples are representative of the structure fluctuations that can occur in real glasses[27] and are used to exemplify an extreme case of a glass with significant local strain and the case of a more homogeneous glass.

2. Theoretical Methodology

The calculations were carried out using two distinct amorphous structures of silica as well as α-quartz and *β*-cristobalite crystalline structures. The amorphous silica structures consisted of 72 atoms in a cubic cell. The quartz structure consisted of 8 unit cells with a total of 72 atoms and that of cristobalite contained 8 unit cells with a total of 96 atoms. All of the systems were subject to periodic boundary conditions.

TABLE 1: The Optimal Configuration and Energy of the Water Dimer Using LDA and GGA[a]

method	$E_{H_{bond}}$	r_{OO}
LDA	−0.411	2.720
GGA	−0.250	2.874

[a] The use of GGA provides a better representation of the water dimer than the LDA when compared to more accurate ab initio calculations.[41]

Both glass structures were generated by classical molecular dynamic (MD) simulations using the BKS potential[28] in the simulation code DL_POLY.[29] The initial structures were made by randomly inserting 24 Si and 48 O atoms into a cubic simulation cell using a suitable distance criteria between atoms to avoid overlaps. The density was fixed at 2.20 g/cm^3 (the experimental average density) during the classical glass-formation simulation. The glass formation was done by first equilibrating the initial random configuration at 7000 K and then quenching the melt in steps to 300 K.[26,30] The quenching rate was about 10^{13} K/s. The final glass structures have all of the Si atoms 4-fold coordinated by O atoms, and all of the O atoms 2-fold coordinated by Si atoms. The two glass samples investigated here were selected from a larger group of glass samples that were shown to have average structures related to a much larger simulated glass.[26] Glasses A and B correspond to glass samples 1 and 4 of ref 26. After annealing, while still using the classical interaction potential, the volumes for glasses A and B were optimized to remove any artificial global strain from the system that could contribute to the increase or decrease of reactivity. Optimized volumes depend significantly on the interaction potential as shown in ref 26. As described in this latter reference, the two glass structures were annealed further and volume optimized using DFT. The optimization procedure is similar to that used by others,[31−33] with the essential difference that the volume optimizations are carried out by scaling the sides of the cell while optimizing the ion positions at each volume until a minimum energy volume is found.[26,30] During optimization, the cell was constrained to be cubic. Further details of the glass generation and structure characterization, including the bond angle distributions, for these and other small silica glass samples are provided in ref 26. The final densities of glasses A and B are 2.33 and 2.26 g/cm^3, respectively. These two glass samples were chosen specifically to investigate the reactions of water in sites having differences in the short- and intermediate-range structure. Other essential differences between the two glass samples are described below.

The DFT calculations were carried out with the VASP code,[34−37] using ultrasoft pseudopotentials,[38] the PW91[39] exchange correlation function, and a plane-wave basis set with an energy cutoff of 29 Ry for the wave function and 68 Ry for the electron density. These calculations used just the Γ point in the *k*-point sampling. The importance of using a generalized gradient approximation (GGA) rather than the local density approximation (LDA) when studying silica has been demonstrated by Hamman.[40] Additional justification for using GGA is obtained by examining the structure and energy of a water dimer. A comparison of the water dimer structure and hydrogen bond energy using LDA and GGA, provided in Table 1, shows that the GGA calculations are comparable to more accurate ab initio calculations.[41]

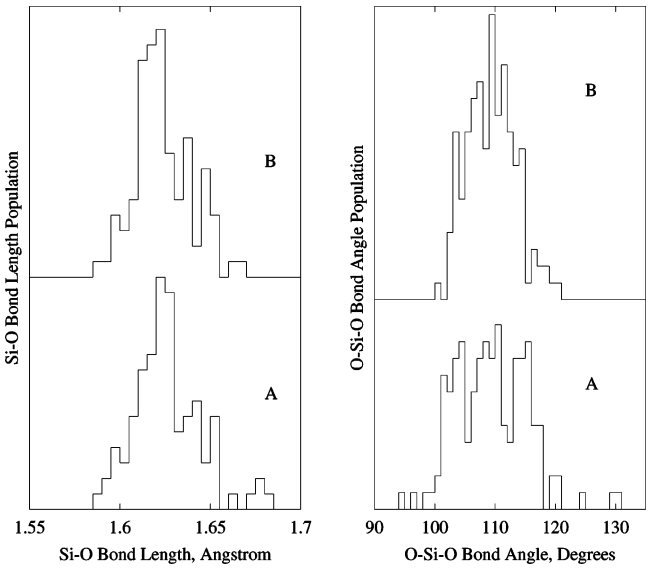

Figure 1. Comparison of short-range structure of glasses A and B. The short-range structure consists of the Si−O bond lengths (on the left) and the O−Si−O bond angles (on the right). The lower histograms are for glass A, and the upper histograms are for glass B. Glass A has wider distributions of Si−O bond lengths and O−Si−O bond angles.

The DFT optimized glass A and B samples differ in that glass A has a wide distribution of Si−O bond lengths and O−Si−O bond angles, whereas, glass B has a more uniform structure, with narrower distributions, as can be seen in Figure 1. The two glass samples are intended to contain representative features of the intermediate-range structure, that is, the ring population and their spatial distributions, found in real glasses. The primitive ring size distribution is wider for glass A than for glass B with both distributions centered about a ring size of 7, counting only the Si atoms. The Si−O−Si bond angle distribution are equally wide with glass B having a larger population at a smaller angle such that the average angles are 145.1 and 146.4°, respectively, for glasses A and B. Note that the data is noisy owing to the small sample, and it is difficult to give a more quantitative analysis. By no means do these two samples contain the entire spectrum of possible local structures, but they do contain local features that are typically found in the medium-range structure of larger simulated glasses that have a total distribution function that is well correlated with neutron diffraction data.[26,30]

The minimum energy path (MEP) and activation barriers of the reaction of a water molecule with the silica network were determined by coupling constant volume DFT calculations with the climbing image-nudged elastic band method (CI-NEB).[42] NEB is a method for finding a minimum energy path between the initial and final states (preferably minima) for diffusion and reaction paths. The climbing-image modification to the NEB method[42−44] ensures convergence to a saddle point along the path. Minimization of the MEP was subject to a convergence criterion of 0.1 eV/Å for the full path and 0.01 eV/Å for the saddle point configuration.

3. Results

3.1. Molecular Water Solvated by the Silica Network. The amorphous network topology of silica glass contains cavities and channels that are nonuniform in size and shape. The intrinsic structure of a cavity can be probed by determining both the response of the network and the energy associated with accommodating an inserted molecule. The effect of having different ring size distributions that lead to different cavity sizes and shapes can also be probed by inserting a molecule into different cavities. It is also necessary to sample the inserted state of a water molecule in the glass samples to obtain a low-energy reference point for the reaction pathway calculations used to determine the reaction activation barriers.

The energy to incorporate a water molecule into the silica network without reaction was determined by inserting water molecules into different cavities of both glasses A and B. There are numerous cavities, even for a small system, of different sizes and shape (they are not necessarily spherical or of some simple geometric shape). In this work, a water molecule was first inserted into a region of the glass to avoid overlap with the atoms of the silica network. The water molecule was then allowed to relax to a local minimum while holding the atoms of the silica network frozen. This was done to avoid artificially breaking the network or inducing some other catastrophic effect. Afterward, the entire system was allowed to relax so that the water molecule could find a deeper local minimum as the network relaxed in response to accommodating the water molecule. Note that there may be several local minima for the water molecule in any given cavity, as described further below. This procedure was repeated to sample several cavities in each of the glass and crystalline systems.

The insertion energy, E_{Insert} is calculated as the difference between the energy of a water molecule inserted into a silica sample and the sum of the energy of the same dry silica sample and the energy of an isolated water molecule. In glass A, the insertion energy was investigated for a series of three densities. At 2.20 g/cm^3, the insertion energy ranged from −0.81 to 2.65 eV. At 2.29 g/cm^3, insertion in the same cavities ranged from −0.66 to 2.77 eV, and at 2.33 g/cm^3 (optimized density of the glass sample) the range was from −0.52 to 2.91 eV. For glass B, the insertion energy at the optimized density of 2.26 g/cm^3 was −0.18 to 0.28 eV.

The broad range of E_{Insert} is correlated with the width of the bond length and bond angle distributions for each glass. For glass A, as the density was increased the insertion energy for each cavity correspondingly increased, and for some cavities the shapes changed so much that the water position in the cavity shifted. Increasing the sample density also led to changes in the hydrogen bonding between the water and the network atoms. However, the width of the range of insertion energy remained fairly constant as the density was changed. This is indicative that in compressing the system volume the intermediate-range structure, that is, the ring and void space distribution, was not affected, although their corresponding conformations did change in response to the volume change as indicated by the shifts in position and hydrogen bonding of the water molecule. In contrast, the more uniform void structure of glass B is revealed by the narrower range of the insertion energy.

For quartz, there is a much narrower insertion energy range of 1.19−1.46 eV, with values similar to previous work.[18] The insertion energy for cristobalite, determined only for a single site (note that cristobalite is highly symmetric and has only one cavity size), was found to be 0.64 eV. The lower value in cristobalite as compared to quartz is due to the lower density and more open structure. Although many of the insertion sites of the glass structures are unfavorable energetically, some insertion sites, as in the more open structure of glass A, can be comparable to the insertion of water into liquid water or ice (the cohesive energy of ice is 0.56 eV).

Water molecules in the cavities of glasses are found in multiple configuration states that include (i) forming hydrogen

bonds between the water molecule and the network oxygen (O_{net}) atoms, (ii) weakly bound or unbound in a relatively large void with the shortest $H-O_{net}$ distance being greater than 2.0 Å, and (iii) covalently bound to a silicon atom of the silica network where the oxygen atom of the water molecule (O_w) has an $Si-O_w$ distance of about 1.8 Å. The bound-state $Si-O_w$ distance of 1.8 Å is in agreement with that found by others in amorphous silica bulk[19] and surface[23] states. Previous work of water in quartz[18] showed unbound and bound molecular water as well. In this work, as shown in more detail below, energy barriers are found between the unbound and bound states for the same cavity.

3.2. Spontaneous Water Reaction in Bulk Silica (Glass A). The initial identification of a Si−O bond site where a water molecule might react most easily was done by carrying out a DFT MD simulation at 1500 K. This was done in glass A by inserting four water molecules into four distinct cavities simultaneously (as determined above) and performing constant temperature molecular dynamics. One water molecule reacted in under 4 ps. A second simulation was run with one water molecule inserted into the same cavity next to the site where the initial reaction took place. This cavity is the most favorable cavity in which to insert water, which is a covalently bound state of water, and for glass A represents a global minimum. An analysis of the void space shows that no other voids have greater volume. During the second simulation, the reaction took place at less than 2 ps. The simulation was stopped immediately after the reaction took place and the reacted system containing a pair of silanol groups was relaxed to its nearest local minimum at 0 K.

The minimum energy path (MEP) was then determined for this reaction path using the NEB method as described above. The first endpoint was that of the inserted molecular water identical to the starting configuration used at the start of the second high-temperature simulation. At 0 K, this endpoint is a molecular water that is covalently bound to the silica network. In this configuration, there is a covalent bond between the oxygen atom of the water molecule and the silicon atom adjacent to the Si−O network bond that gets ruptured during reaction. The second endpoint was that of the relaxed silanol configuration obtained at the end of the second high-temperature simulation. A series of eight images were interpolated between the two endpoints to form a reaction path, and the path was optimized using the DFT-NEB method. The same path was determined for three different densities corresponding to the initial configuration at a density of 2.20 g/cm^3, the optimized density of 2.33 g/cm^3, and one in between corresponding to 2.29 g/cm^3. The resulting MEPs are shown in Figure 2. The changes in the barrier height and relative stability of the reactant and product states illustrate the nature and magnitude of the errors that can be introduced when the configuration is not optimized with respect to the interaction potential.

In glass A for this particular reaction site and at the optimized density (2.33 g/cm^3), the molecular water (reactant) state is less stable than the silanol (product) state by 1.9 eV and the forward reaction has an activation barrier of less than 0.2 eV. The activation barrier is observed to decrease as the density gets lower (going away from the optimized density) and occurs sooner along the MEP. Correspondingly, the difference in energy between the reactant and product states increases. The nonoptimized configurations have different degrees of network relaxation that are responsible for the shifts in the activation barrier and the relative stability of the product and reactant states. Although it seems unusual that a water molecule would react

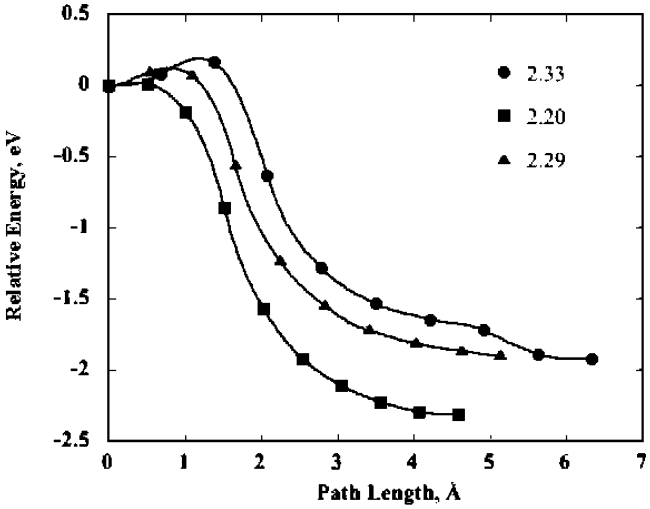

Figure 2. The MEP for the reaction of a water molecule with a strained site in the network of glass A. The different curves correspond to the same MEP at three different densities: 2.33, 2.29, and 2.20 g/cm^3 from top to bottom, respectively. The three curves are normalized to set the initial molecular water state at zero. At the lowest density, the reaction barrier is 0.03 eV, and the silanol group configuration is stabilized by 2.32 eV with respect to the molecular water.

with such a low activation barrier in bulk silica, this reaction is likely to have occurred already during processing of a glass in the presence of water, and thus would not necessarily be measured during a diffusion experiment. To gain an understanding of the effect of this nearly spontaneous reaction, and the stability of the product state as compared to the molecular water state, we made an analysis of the network structure as a progression from the dry glass, to the water inserted glass, and finally to the reacted glass.

The response of the Si−O bond length, the O−Si−O bond angle, and the Si−O−Si bond angle along the reaction path was determined by monitoring the perturbation of the bond lengths and angles in each of the different states. A correlation is found in the network response in terms of the Si−O bond length and the O−Si−O bond angles. No correlation of the reaction site with the Si−O−Si bond angle distribution was found.

Scatter plots of the O−Si−O bond angle versus Si−O bond length for the dry glass, molecular water state, and silanol state configurations are shown in Figure 3. In these plots, each bond length is associated with three bond angles when the Si atom forms a tetrahedron with the neighboring O atoms. In this particular case, the inserted molecular water is covalently bound to a silicon atom, so that one Si atom is bound to five O atoms. On the 5-fold coordinated Si atom, each bond length corresponds to having four bond angles, as is shown in the center frame of Figure 3, where the four bond angles for a the bond length corresponding to the Si−O bond that is broken are marked with ◊ and those corresponding to the Si−O bond formed with the water molecule are marked with ⊕.

The following features are identified from the scatter plot of Figure 3. The reaction site in the dry glass is found to have the longest bond length and the widest bond angle and is marked with filled diamonds in the top frame of Figure 3. In addition, the reaction site also contains a narrow bond angle that, along with the wide bond angle, is relaxed when the bond is ruptured. The insertion of water stretches the local structure while forming a 5-fold coordinated Si atom. Note that the bond angle scale is expanded for the molecular water inserted state. Finally, in comparison to the dry glass, the silanol state has a more compact

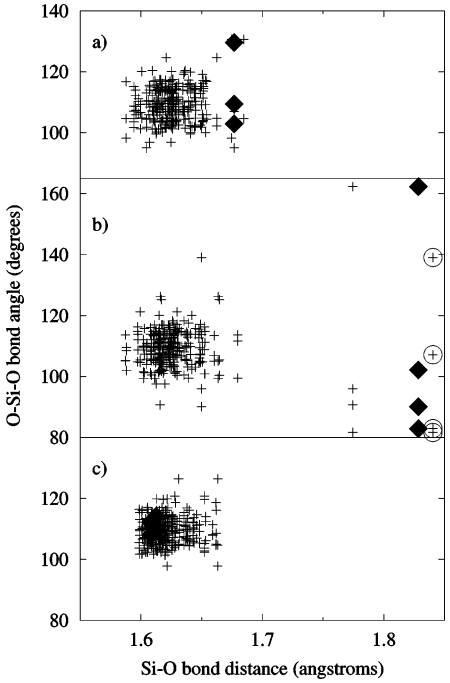

Figure 3. Plots of the bond angle versus bond length in (a) dry glass A, (b) glass A with an inserted molecular water, and (c) relaxed glass A with silanol groups, as in Figure 2. Each bond length is associated with three bond angles for a 4-fold coordinated Si atom and four bond angles for a 5-fold coordinated Si atom. The Si−O bond that breaks is indicated by filled diamonds. The angles formed by the Si−O bond including the water molecule are indicated by ⊕. After reaction with a water molecule, there is noticeable compaction in the scatter of bond lengths and angles, indicating significant relaxation of the silica network.

distribution. The compaction of the distribution is an indication that depolymerizaton of the network leads to the release of local network strain, and annealing-like behavior, which contributes to the stabilization of the silanol pair. The strained site is correlated with the most favorable insertion energy for molecular water in a bound state and a low activation barrier for hydrolysis. The wide bond angle of the dry glass configuration allows the water to approach easily and enter into a bound state. In contrast, the approach of the water molecule from the other side, toward the narrow bond angle, is hindered, and the activation barrier is expected to be significantly higher. The dependence on the approach of a water molecule to a reaction site is demonstrated for glass B below. The Si site that is subject to attack in this reaction is adjacent to a four-membered ring (where an *N*-membered ring contains *N* Si atoms), and the ruptured bond is part of a kinked site in a five-membered ring.

3.3. Water Diffusion and Oxygen Atom Exchange by Reaction (Glass B). The bond length−bond angle structure analysis for the dry glass B configuration was used to identify a reaction site similar to the site found for glass A, namely, one where a long Si−O bond length is associated with a wide O−Si−O bond angle. As in glass A, the Si atom associated with the identified reaction site participates in a four-membered ring, but the bond that breaks does not participate in that ring. The initial reactant state was prepared by breaking the chosen long Si−O bond and inserting a dissociated water molecule to create a pair of silanol groups across the severed bond. In determining the complete MEPs discussed and shown below, it was often necessary to add more images to the NEB calculations to obtain more detail as different extremum points were discovered. In general, there are no less than six images between minima separated by the lowest-lying barriers and at least eight images between minima separated by the highest-lying barriers.

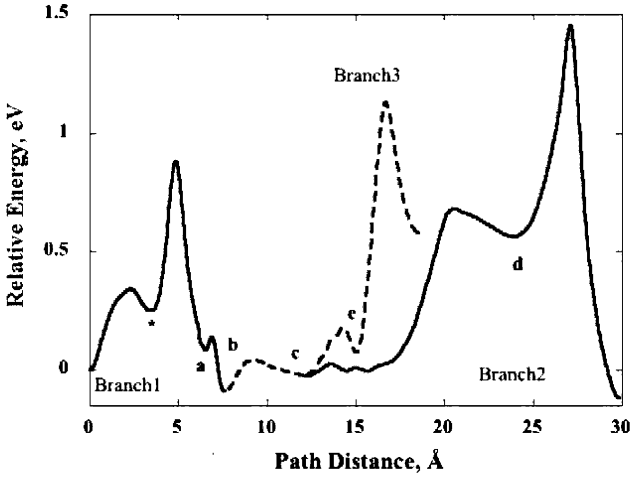

Figure 4. The branched MEP for the reaction of water in glass B. The solid and dashed portions of the curve indicate opposite directionality of the OH groups, which results in a different oxygen atom incorporated into the molecular water state. This means that a path including both a solid and a dashed branch results in an exchange of an oxygen atom between the water molecule and the silica network. At the end of each branch, the water is in a molecular state. The silanol group conformations, labeled a−e, are shown in Figure 6, and the molecular water conformations are shown in Figure 5. On branch 1, the bound molecular water state is indicated by an asterisk.

Two distinct cavities adjacent to the chosen Si−O bond reaction site provided the molecular water state configurations for two independent reaction MEPs to the same site. These inserted water states are not the global minimum for this sample, but are close to energetically neutral, with insertion energies of less than ±0.1 eV. The two resulting MEPs, labeled as branch 1 and branch 2 in Figure 4, form a diffusion path between the two molecular water states via a reaction of the water molecule with the silica network, without an exchange of the oxygen atom. At the path endpoints of branch 1 and branch 2, the water molecule is unbound in the cavity. The unbound molecular water at the start of branch 1 (see Figure 5) is used as the reference state for the paths presented for glass B in Figure 4. The molecular water state of branch 2 is lower in energy than the molecular water state of branch 1 by about 0.1 eV. The molecular water conformations are shown in Figure 5.

In branch 1, the unbound water goes over a barrier of about 0.4 eV to a bound molecular water state. The path from the bound molecular water state to a silanol reacted state, labeled as H_a, has a barrier of 0.65 eV. The formation energy between the initial unbound molecular water state and this silanol state is about 0 eV. For this reaction site in glass B, the silanol group pair has a number of different local minimum conformations, related by rotations of the OH groups, and minor shifts or twists in the surrounding silica lattice. The five silanol conformations found are shown in Figure 6. A rotational rearrangement of one OH group, with a barrier of less than 0.10 eV, leads from H_a to a lower energy conformation labeled H_b, where the protons point in opposite directions away from each other. The H_b conformation has the lowest configuration energy along this path and is lower than the unbound molecular water state at the beginning of branch 1 (the reference state). Another conformation change can take place from H_b to H_c, with a barrier of 0.17 eV, in which the silanol group pair have undergone a 180° rotation with respect to conformation H_a and have exchanged their roles as hydrogen bond donor and acceptor. Following branch 2, starting from H_c the silanol groups undergo a more complicated

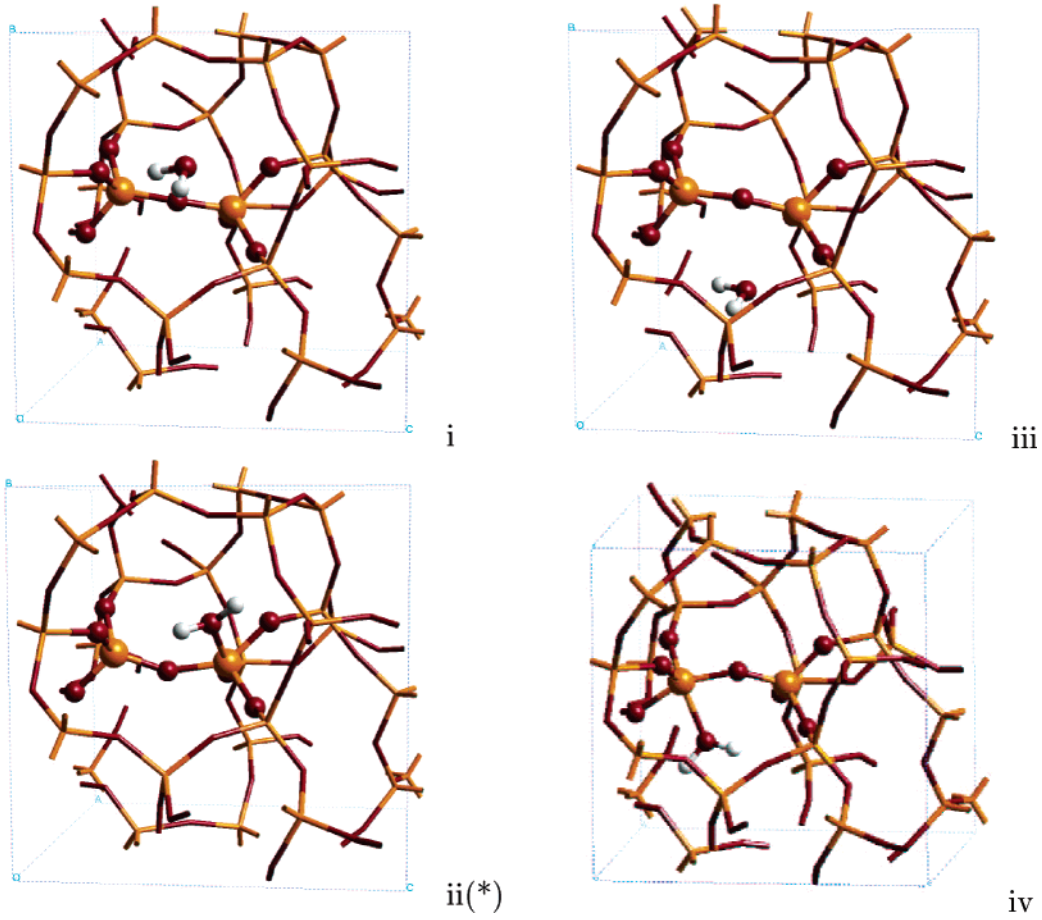

Figure 5. Some of the major conformations of molecular water found in the reaction−diffusion paths in glass B corresponding to the MEP in Figure 4. Silicon atoms are shown in orange, and oxygen atoms are shown in red. Hydrogen atoms are white. For clarity, only the atoms immediately involved in the reaction are shown as spheres. Configurations i and iii correspond to the endpoints of branches 1 and 2, respectively. Configuration ii(*) shows the atom positions for the intermediate bound state for molecular water that occurs in branch 1. Finally, configuration iv corresponds to the endpoint of branch 3.

conformation change to a higher energy (more strained) conformation labeled as H_d, with a barrier of 1.07 eV. There are other minor configurational changes between H_c and H_d with OH conformations similar to those of H_c. From the H_d conformation there is a 0.93 eV barrier to an unbound molecular water state in a cavity opposite the starting point of branch 1.

The H_e conformation of the silanol groups is shown in Figure 6e. The configuration energy and the conformation is very similar to H_c, with a small twist of the surrounding silica network. The barrier from the H_c to the H_e state is about 0.12 eV. The path from H_e to the end of branch 3 leads to the formation of a bound molecular water state, with a barrier of 1.07 eV. The bound molecular water is in the same cavity as the unbound molecular water state of branch 2 (see Figure 5). There is a barrier to the unbound state similar to that seen along the path of branch 1. Following a path from either branch 1 or branch 2 through branch 3 results in the exchange of a network oxygen atom with the water molecule.

3.4. Diffusion of Molecular Water by Reaction in Crystalline Silica. A diffusion-reaction path between a small and large cavity in α-quartz was investigated, and the MEP is shown in Figure 7. The NEB path had eight intermediate images between minima. The activation barrier from the first cavity (the reference state for this MEP) is 1.06 eV. The barrier from the second cavity into the same reacted state is 1.25 eV. The activation barriers from the reacted state are 0.44 and 0.65 eV to the first and second molecular water states, respectively. Along this MEP, no exchange of the O atom occurs. Although a rotation of the OH groups is possible, such as that between H_a and H_c of glass B, only one stable conformation was found for the silanol pair in the crystal.

Along one branch of the quartz reaction path, calculations were carried out to determine the evolution of the charge state as the reaction progressed. The calculations were carried out with the CASTEP code[45] using GGA-PW91. Single-point calculations were carried out where images of the reaction sequence were taken from the VASP-NEB MEP. A Mulliken charge analysis of the results showed an average charge on the O atoms of the network of −1.18 and for the Si atoms the average charge was +2.36. These values of the charge state are in agreement with other work.[28,46] In the inserted molecular water, the O was −0.92 with the H atoms having a charge of +0.48. There is charge transfer between the protons of the inserted molecular water and the network O atoms with which it forms hydrogen bonds, and so the network O atoms participating in the hydrogen bonding are slightly more negative than O atoms elsewhere in the silica network. Each system conformation, especially between the unbound and bound states of the water molecule, has a different charge distribution for the O and H atoms of the water molecule and the O and Si atoms that participate in hydrogen bonding and in 5-fold coordinated states, respectively. As the reaction progresses, the charge on the O atom of the water and the O atom in the Si−O bond that ruptures, slowly change to a final charge of −1.05. There is a small change in charge of the H to +0.49. The Si atoms have significant charge fluctuations because small changes

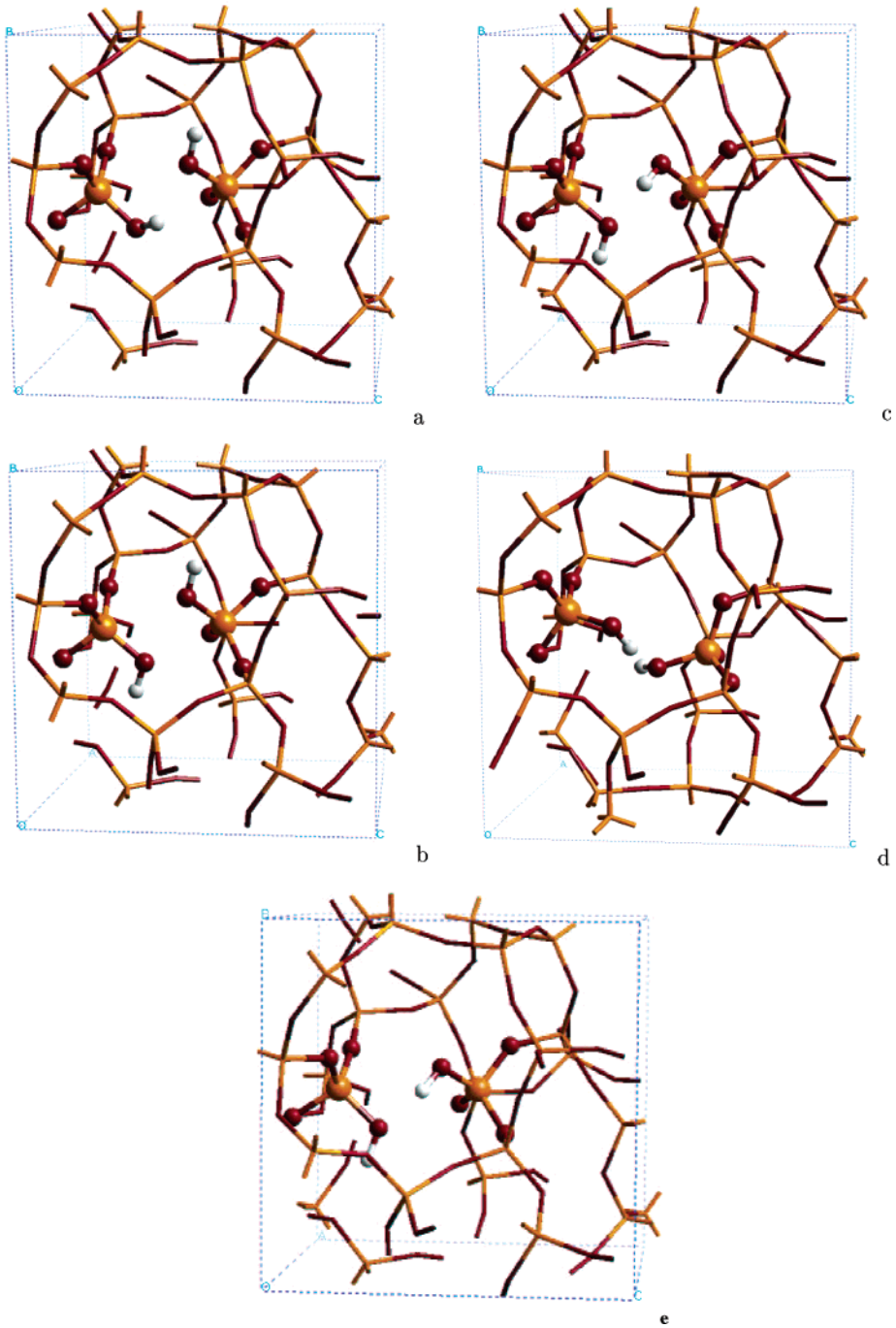

Figure 6. Some of the major conformations of the silanol groups found in the reaction−diffusion paths in glass B corresponding to the MEPs in Figure 4. The colors and representation of the atoms is the same as in Figure 5. The labels a−e correspond to the similarly marked points on Figure 4. The different states are made possible by small barriers to rotation for the individual O−H groups into nearby local minima. Configuration d requires more accommodating motion from the surrounding network, which is consistent with the significantly higher energy for this local minimum.

in the Si−O distances and O−Si−O bond angles cause changes of about on average ±0.05 in the charge state.

A reacted state of water in cristobalite was also examined. Upon rupturing an Si−O bond in cristobalite to create a pair of silanol groups, the low energy state is found to be an edge-sharing configuration in which the protons are attached to 3-fold coordinated O atoms, also connected to the Si atoms. The bonds from the 3-fold coordinated O atoms to each of the Si atoms are asymmetric. The activation barrier is estimated to be above 2 eV, where the MEP to this particular configuration from a molecular water state is rather complex. Although there may be many intermediate states between these two endpoints, the overall reaction path is uphill with an energy difference of 0.58 eV, which is about the same as that for quartz.

4. Discussion

A wide range of incorporation energy for the insertion of water into a cavity was found for glass A. Glass A exhibits considerable local strain, and may be considered more closely related to a poorly annealed glass owing to its higher density, more open structure, and a broad distribution of the intermediate-range structure. The most favorable insertion configurations are those in which the cavity is open and flexible enough to allow the water molecule to form a covalent bond between the O_w

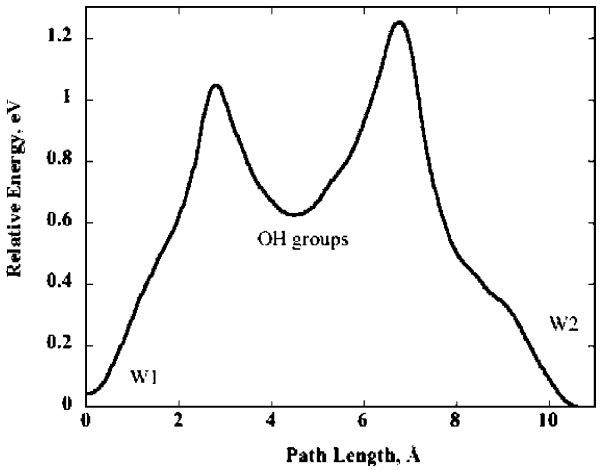

Figure 7. Diffusion reaction path in quartz. At W1 and W2, the water is in a molecular state. The local minimum in the middle of the path corresponds to a configuration in which a network bond has been broken; the water has been inserted to form two OH groups. Only one stable silanol group conformation was found for quartz.

atom of the water molecule and an Si atom of the network. This work shows that the presence of local strain at a tetrahedral site is very important. Strain that causes wide angles and longer bonds acts to decrease the repulsion between the oxygen atoms of the water molecule and the silica network so that the water may approach and form a covalent $Si-O_w$ bond.

The energy gained through the formation of an $Si-O_w$ bond can compensate for the induced strain in the silica network. In smaller, less flexible cavities, the bound water molecule can be a local minimum that is higher than the unbound water molecule. Such is the case for glass B. Glass B may be considered a "better" glass because it has a lower density, shows a more uniform structure, and has an intermediate-range structure more closely related to what is expected to be a good glass.[26] The more uniform cavity sizes are revealed by the narrower range of insertion energy determined for this glass sample. In comparison to other work, the overall range of insertion energy of both glasses A and B are similar to those found in ref 20, where the smaller voids found in glass A have a high insertion energy similar to the smaller 4.5−4.0 Å voids of that reference. In contrast, our glass A also contains a much larger and more flexible void that leads to a significantly lower insertion energy. The voids are more uniform in glass B where the insertion energy range corresponds to the void sizes between 7 Å and greater than 5 Å of ref 20. The energy difference between the bound and unbound states of our glass B are also related to those of ref 20, indicating that our glass B is similar to that glass sample.

The results for glass B, a more representative sample, show that the activation barrier in a glass can be even higher than that in quartz, which does not uptake water readily, while also providing barriers that are lower than those in quartz. In contrast, we find that glass A has a significantly lower reaction barrrier at one specific reaction site so as to capture and retain water in the form of silanol groups. This site is highly reactive as compared to the experimental activation barrier, and the activation barriers found for glass B. A reaction site like this is likely to be annealed by hydrogen or OH capture during processing or is representative of a rare site in a good glass. From the two extreme examples, glass A and B, we find that the extent of the network response plays a major role in the stability of the reactants and products, and, consequently, on the activation barrier. In glass A, the local network configuration favors the silanol groups over maintaining a strained configuration. Strain is considered in terms of the relative energy of the configurations and as a function of how stretched the bond lengths and how wide the O−Si−O bond angles are relative to the equilibrium or ideal crystal-like configuration. The resistance of the network to reforming a water molecule reveals a factor that controls the retention of water in glass, namely, that the reaction of water with silica can anneal the network structure. When a water molecule reacts at a strained site, the activation barrier is low and the glass network relaxes to remove strain from the system. In turn, the number of strained bond lengths and bond angles is reduced, as indicated by the dramatic decrease in the scatter of the Si−O bond length and O−Si−O bond angles seen for glass A. We observe that relaxation of unusually narrow angles also occurs.

When the reaction-induced annealing process occurs, it can be expected that reactions at other nearby sites become less likely as the structure relaxes to become locally more ideal. Thus, the reaction activation barriers of glass A can become more like those seen for glass B. In contrast, reaction at an unfavorable site, that is, one where the stability of the silanols is higher than that of the molecular water, results in the addition of strain to the network that can create sites more susceptible to reaction. A collection of the latter mechanism contributes to hydrolytic weakening processes.

The overall activation energies determined for glass B are similar to those determined in previous work.[19] Relaxation of strain in the surrounding network stabilizes the silanol groups relative to the molecular water state, but only slightly. The relaxation is enough to allow the silanol configuration to be similar in energy to the free molecular water configuration, rather than significantly higher, as in crystalline silica. The lowest energy configuration of the silanol groups is found to be the one in which no hydrogen bonding between the OH groups exists. This is related to experimental work that shows little if any signal of hydrogen bonding between OH groups in silica glass.[47] Furthermore, the relaxation of the network also acts as an annealing process for glass B, although it is a much smaller effect than that for glass A.

We found that the reactivity at a distorted site allowed the water molecule to approach the Si atom more easily because of the wide O−Si−O angle. Wider bond angles and longer bonds can reduce the steric hindrance by minimizing the repulsion between the O atoms of the water and the network. As seen in glass B, the ease of reaction can vary according to the direction of approach for the same silicon site in the lattice. This effect is probably due to geometrical constraints because an Si site with a wide bond angle will likely have a narrow bond angle as well. An approach to a strained site from the direction of a narrow bond angle can result in a reaction barrier higher than that for crystalline silica. As seen in glass B, a reaction approaching from the less favorable direction may also have a relatively high-energy initial silanol conformation that can relax to other conformations. In this case, an examination of the structure (see Figure 6) shows that accommodation of the silanol groups requires significant twisting of the surrounding network, which adds additional strain, rather than relieving it. Unlike the case of quartz, however, the silanol groups in glass B can pass over a relatively small barrier to reach several lower energy conformations. Rotation between different conformations within the low-energy silanol "envelope" has very little effect on the surrounding network. If quantum/zero-point energy is considered, then the OH groups may be able to rotate even at room temperature. The ease of this rotation is important in the

rate of oxygen exchange between water molecules and the silica network because the rotational state that links to the exchange MEP must be sampled for that reaction to occur. The existence of multiple nearly degenerate states of the silanol groups can have the effect of reducing the reaction rate back toward forming molecular water because multiple nearly degenerate silanol conformations increase the density of states for the silanol side of the MEP. The increase in the density of states enters into the prefactor of the rate constant and not into the activation barrier. As long as the reaction activation barriers and associated mechanisms are similar for diffusion by reaction and for exchange, then there will be little differences in the observed rates of reaction. Many more reaction paths would have to be sampled to determine the statistical distribution of the activation barriers for both diffusion and exchange paths.

Examination of the reaction pathways for both the glasses and the silica crystals shows that in cases where the water can approach and form a bound state to the silica lattice the barrier to reaction is significantly lower. This bound state may be considered an important precursor to reaction. This has not been revealed previously by ab initio cluster calculations. For glass B, the bound state is an intermediate local minimum (also seen in ref 20), whereas in glass A, the bound state is lower in energy than any free water configuration found in that glass.

No systematic attempt was made to investigate the role of ring size on the reaction barriers. In this work, no small rings are ruptured. Although the reaction site in each glass is adjacent to a four-membered ring, the actual strained bond is associated with a kink of a larger ring. The adjacency of the four-membered ring to a large ring may be correlated, but more importantly, it is *not* the rupture of the four-membered ring that leads to a large relaxation in glass A. The strain associated with an ideal four-membered ring is expected to be about 0.02 eV,[48] which is relatively small. Although smaller rings are predicted to have additional strain, neither of the investigated glasses had any two- or three-membered rings. Although studies of sol−gel reactions show that small rings are more reactive at the sample surface,[21,22] recent bulk calculations state that the formation energy of silanol group pairs is more favorable for larger (six- and eight-membered) rings.[20] Scission of a small ring may potentially reduce the strain associated with that small ring, but the rupture of a bond in a larger ring may allow a longer range relaxation involving folding or unfolding of the long network chain structure associated with the large ring. In addition, although breaking a bond allows the strain to relax, formation of the silanol groups also requires room to fit across the broken bond. Further work to investigate the effect of ring size more directly would be useful.

Finally, understanding how the charge of the individual ions changes when bonds are ruptured and reformed into different molecular components is important for the development of classical potentials for use in large-scale simulations of glass structure.[49] The charge analysis shows that the charge state of molecular water is modified with the hydrogen bonding with the network. Although these changes are subtle, they do represent important changes in the chemical environment and go beyond simple packing interactions.[50] More detailed work would be valuable to determine the role of polarization and of higher moments[51] in this and related materials.

5. Conclusions

The role of network response in the reaction of molecular water with amorphous states of silica was determined using two extreme examples that represent a locally strained glass, and a more uniformly annealed glass. In both cases, the degree of network relaxation leads to stabilizing either the molecular water or the silanol states. It is likely that highly reactive sites such as those found in glass A react early on in the processing stages as long as there is water or some other small molecule with which it can react and are otherwise rare in good glasses. The highly reactive site is found to be due to strain in the network that can trap the water in the form of silanol groups as a result of annealing the local network. In contrast, a more uniform (perhaps better) glass, such as that represented by glass B, can have a reaction site that leads to diffusion and exchange of an O atom where the network response is minimal and the reactant and product states have nearly identical energies. A higher barrier can exist in silica glass, as compared to quartz, however, the relative stability of the two states can approach zero owing to additional conformations of the silanol state to lower energy configurations. The latter is not possible in a pristine crystal, but could occur near defects and at grain boundaries.

Acknowledgment. This work was supported by the Office of Basic Energy Science, U.S. Department of Energy. The research was carried out at the University of Washington and at the William R. Wiley Environmental Molecular Sciences Laboratory, a national scientific user facility sponsored by the U.S. Department of Energy, Office of Biological and Environmental Research located at Pacific Northwest National Laboratory. Battelle operates the Pacific Northwest National Laboratory for the U.S. Department of Energy.

References and Notes

(1) Moulson, A. J.; Roberts, J. P. *Trans. Faraday Soc.* **1961**, *57*, 1208.
(2) Doremus, R. H. *J. Mater. Res.* **1995**, *10*, 2379.
(3) Baer, D. R.; Pederson, L. R.; McVay, G. L. *J. Vac. Sci. Technol., A* **1984**, *2*, 738.
(4) Roberts, G. J.; Roberts, J. P. *Phys. Chem. Glasses* **1966**, *7*, 82.
(5) Pfeffer, R.; Ohring, M. *J. Appl. Phys.* **1981**, *522*, 777.
(6) Brinker, C. J.; Scherer, G. W. *J. Non-Cryst. Solids* **1985**, *70*, 301.
(7) Gross, A.F.; Le, V. H.; Kirsch, B. L.; Tolbert, S. H. *J. Am. Chem. Soc.* **2002**, *124*, 3113.
(8) Drury, T.; Roberts, J. P. *Phys. Chem. Glasses* **1963**, *4*, 79.
(9) Mikkelsen, J. C. *Appl. Phys. Lett.* **1981**, *39*, 903.
(10) Roberts, G. J.; Roberts, J. P. *Phys. Chem. Glasses* **1964**, *5*, 26.
(11) Tomozawa, M.; Li, H.; Davis, K. M. *J. Non-Cryst. Solids* **1994**, *179*, 162.
(12) Davis, K. M.; Tomozawa, M. *J. Non-Cryst. Solids* **1995**, *185*, 203.
(13) Tomozawa, M.; Kim, D.-L.; Agarwal, A.; Davis, K. M. *J. Non-Cryst. Solids* **2001**, *288*, 73.
(14) Uglienko, P.; Saunders, V.; Garrone, E. *J. Phys. Chem.* **1990**, *94*, 2260.
(15) Lasaga, A. C.; Gibbs, G. V. *Am. J. Sci.* **1990**, *290*, 263.
(16) Heggie, M.; Jones, R. *Philos. Mag. Lett.* **1987**, *55*, 47.
(17) Hagon, J. P.; Stoneham, A. M.; Jaros, M. *Philos. Mag. B* **1987**, *55*, 225.
(18) Jones, R.; Oberg, S.; Heggie, M. I.; Tole, P. *Philos. Mag. Lett.* **1992**, *66*, 61.
(19) Bakos, T.; Rashkeev, S. N.; Pantelides, S. T. *Phys. Rev. Lett.* **2002**, *88*, 05508.
(20) Bakos, T.; Rashkeev, S. N.; Pantelides, S. T. *Phys. Rev. B* **2004**, *69*, 195206.
(21) Brinker, C. J.; Tallant, D. R.; Roth, E. P.; Ashley C. S. *J. Non-Cryst. Solids* **1986**, *82*, 117.
(22) Brinker, C. J.; Kirkpatrick, R. J.; Tallant, D. R.; Bunker, B. C.; Montez, B. *J. Non-Cryst. Solids* **1988**, *99*, 418.
(23) Du, M. H.; Kolchin, A.; Ping, H.-P. *J. Chem. Phys.* **2002**, *120*, 1044.
(24) Hammond, G. S. *J. Am. Chem. Soc.* **1955**, *77*, 334.
(25) Ceresoli, D., Bernasconi, M.; Iarlori, S.; Parrinello, M.; Tossatti, E. *Phys. Rev. Lett.* **2000**, *84*, 3887.
(26) Van Ginhoven, R. M.; Jónsson, H.; Corrales, L. R. *Phys. Rev. B.* **2004**, *71*, 024208.
(27) Varshneya, A. K. *Fundamentals of Inorganic Glass*; Academic Press: San Diego, 1994; Chapter 13.
(28) van Beest, B. H. W.; Kramer, G. J.; van Santen, R. A. *Phys. Rev. Lett.* **1990**, *64*, 1955.

(29) Smith, W.; Forester, T. *J. Mol. Graphics* **1996**, *14*, 136.
(30) Van Ginhoven, R. M. PhD Thesis, University of Washington, Seattle, WA, 2002.
(31) Benoit, M.; Ispas, S.; Jund, P.; Jullien, R. *Eur. Phys. J. B* **2000**, *13*, 631.
(32) Ispas, S.; Benoit, M.; Jund, P.; Julien, R. *Phys. Rev. B* **2001**, *64*, 214206.
(33) Szymanski, M. A.; Shluger, A. L.; Stoneham, A. M. *Phys. Rev. B* **2001**, *66*, 224207.
(34) Kresse, G.; Hafner, J. *Phys. Rev. B* **1993**, *47*, 558.
(35) Kresse, G.; Hafner, J. *Phys. Rev. B* **1994**, *49*, 14251.
(36) Kresse, G.; Furthmuller, J. *Comput. Math. Sci*. **1996**, *6*, 15.
(37) Kresse, G.; Furthmuller, J. *Phys. Rev. B* **1996**, *54*, 11169.
(38) Vanderbilt, D. *Phys. Rev. Lett.* **1990**, *41*, 7892.
(39) Perdew, J. In *Electronic Structure of Sol.*; Ziesche, P., Eschrig, H. Eds.; Akademie Verlag: Berlin, Germany, 1991.
(40) Hamman, D. R. *Phys. Rev. Lett.* **1998**, *81*, 3447.
(41) Xantheas, S. S. *J. Chem. Phys.* **1995**, *102*, 4505.
(42) Henkelman, G.; Uberuaga, B. P.; Jónsson, H. *J. Chem. Phys.* **2000**, *113*, 9978.
(43) Mills, G.; Jónsson, H.; Schenter, G. K. *Surf. Sci.* **1995**, *324*, 305.
(44) Mills, G.; Jónsson, H.; Jacobsen, K. W. In *Clasical and Quantum Dynamics in Condensed Phases*; Ciccotti, G.; Berne, B. J.; Coker, D. F., Eds.; World Scientific: Singapore, 1998; Chapter 16.
(45) Computational results obained using CASTEP currently distributed by Accelrys Inc. as part of the Cerius^2 molecular modeling system.
(46) Tsuneyuki, S.; Tsukada, M.; Aoki, H.; Matsui, Y. *Phys. Rev. Lett.* **1988**, *61*, 869.
(47) Adams, R. V.; Douglas, R. W. *J. Soc. Glass Technol.* **1959**, *43*, 147.
(48) Uchino, T.; Kitigawa, K.; Yoko, T. *Phys. Rev. B* **2000**, *61*, 234.
(49) Du, J.; Cormack, A. N. *J. Am. Ceram. Soc*., in press, 2005.
(50) Wright, K.; Catlow, C R. A. *Phys. Chem. Miner.* **1994**, *20*, 515.
(51) Batista, E.; Xantheas, S. S.; Jónsson, H. *J. Chem. Phys.* **2000**, *112*, 3285.